JOURNAL OF AGRICULTURAL AND FOOD CHEMISTRY

ARTICLE

pubs.acs.org/JAFC

Bovine Serum Albumin Nanoparticle Promotes the Stability of Quercetin in Simulated Intestinal Fluid

Ru Fang, Ruifang Hao, Xia Wu, Qi Li, Xiaojing Leng,* and Hao Jing*

College of Food Science and Nutritional Engineering, China Agricultural University, Key Laboratory of Functional Dairy Science of Beijing and Ministry of Education, Beijing Higher Institution Engineering Research Center of Animal Product, No. 17 Qinghua East Road, Haidian, Beijing 100083, China

ABSTRACT: Quercetin (Que) is a flavonoid widely distributed in vegetables and fruits and exhibits strong antioxidant activity, but the poor stability of Que limits its function and application. The present study developed a nanoparticle (NP) using bovine serum albumin (BSA) as a matrix to encapsulate Que. The stability of encapsulated Que by BSA NP was tracked in a simulated intestinal fluid (SIF). The antioxidant activity of encapsulated Que was evaluated by the 2,2-diphenyl-1-picrylhydrazyl (DPPH) and 2,2′-azinobis(3-ethylbenzothiazoline-6-sulfonic acid) (ABTS) radical scavenging assays. Furthermore, the stabilizing mechanism of Que by BSA NP was investigated, using scanning transmisson electron microscopy (STEM), dynamic light scattering (DLS), UV−vis, fluorescence spectrometry, and circular dichroism (CD). The results revealed that Que was effectively encapsulated by BSA and formed spherical NP (<10 nm). BSA NP not only promoted the stability of encapsulated Que but also kept the antioxidant activity of encapsulated Que. The driving forces for BSA−Que association were hydrophobic interaction and hydrogen bond, and the latter was involved in the mechanism of Que stabilization. This suggested that BSA NP could be a good carrier to deliver hydrophobic flavonols.

KEYWORDS: bovine serum albumin, nanoparticle, quercetin, stability, antioxidant activity

INTRODUCTION

Quercetin (Que) is widely distributed in vegetables and fruits and is an important dietary source of flavonols. Que exhibits antioxidant, anticancer, and antiviral activities,[1] but the poor stability of Que restricts its function and application. Que was easily oxidized and formed Que *o*-quinone/*o*-quinone methide (QQ), which was associated with its reactive hydroxyl groups.[2,3] The half-life of Que was <10 h in potassium phosphate buffer (0.1 M, pH 7.4) and 2 h in McCoy's 5A culture medium.[2] The low stability and poor solubility lead to extremely low bioavailability of Que. To overcome these problems, an encapsulation system, especially a nanocapsule, has attracted a great deal of attention. A nanoparticle (NP) has been shown to improve the stability and solubility of some small molecular compounds.[4]

Some synthetic or natural macromolecules (polymers, proteins, polysaccharides, and liposomes) were used to prepare NP. Bovine serum albumin (BSA) is an attractive natural protein and has been a subject of major interest in micro- or nanoencapsulation. Using a coacervation process, that is, desolation with ethanol and then solidification with glutaraldehyde, BSA could form NP and deliver the hydrophilic compounds such as phosphodiester oligonucleotide, 5-fluorouracil, and sodium ferulate.[5,6] Due to its flexibility in structure, together with the charges differently distributed along the molecule, BSA can bind many compounds with different structures. It was reported that BSA bound hydrophobic anionic compounds through its site I,[7] which is a specific site for binding nonsteroidal hydrophobics because hydrophobicity of tryptophan (Trp) existed in the hydrophobic pocket of site I.[8] Although some studies had reported that Que interacted with BSA through hydrophobic interaction or hydrogen bond,[9,10] the driving force for the interaction and their contribution to the stability of Que were not clear.

The present study aims to design a BSA NP with a size smaller than 10 nm to encapulate Que and promote its stability. The stability as well as the antioxidant property of encapsulated Que was evaluated. Furthermore, the driving force for the interaction of BSA and Que and their contribution to the stability of Que were investigated.

MATERIALS AND METHODS

Chemicals. BSA (fraction V, purity = 98%) (A-0332) was purchased from AMRESCO (Amresco Inc., Solon, OH). 1-Diphenyl-2-picrylhydrazyl (DPPH, D9132-1G), 2,2′-azinobis(3-ethylbenzothiazoline-6-sulfonic acid) diammonium salt (ABTS, A-1888), pancreatin (8 × USP specifications, P7545), and dimethyl sulfoxide (DMSO; purity = 99.5%) were all purchased from Sigma-Aldrich, Inc. (St. Louis, MO). Que (3,3′,4′,5,7-pentahydroxyflavone hydrate) (Q-100081; purity = 97.3%, HPLC grade) was purchased from National Institute for the Control of Pharmaceutical and Biological Products (Beijing, China). All other reagents used were of analytical grade.

Preparation of Que-Loaded BSA NP Solution. The stock solution of BSA (1.5×10^{-3} mol/L) was prepared with Milli-Q water. The stock solution of Que (1.5×10^{-3} mol/L) was prepared with DMSO, one of the most versatile organic solvents. Both stock solutions were stored in the refrigerator at 4 °C prior to use. The Que-loaded BSA NP solution was prepared as follows: Que stock solution was added to

Received: February 20, 2011
Revised: May 4, 2011
Accepted: May 4, 2011
Published: May 04, 2011

diluted BSA stock solution, mixing on a vortex thoroughly for 5 min. The final concentrations of BSA and Que were 1.5×10^{-5} and 1.5×10^{-4} mol/L, respectively, and DMSO was 10% (v/v).

Scanning Transmisson Electron Microscopy (STEM). The Que-loaded BSA NP powder was obtained by freeze-drying to remove DMSO. The native BSA and lyophilized Que-loaded BSA NP were dissolved in Milli-Q water to prepare the test solutions at the concentration of BSA at 1.5×10^{-5} mol/L. The solution (10 μL) was cast onto a copper TEM grid for 5 s, and then the redundant solutions were absorbed with filter paper. After 10 min, the phosphotungstic acid solutions (0.2 mol/L, pH 7.0) were cast onto copper TEM grids and stained for 10 min, and then redundant solutions were absorbed with filter paper. After 10 min, the dried copper grids were kept in the desiccator before observation. The dried copper grids were observed on a Hitachi S-5500 STEM (Hitachi High-Technologies America, Inc., Schaumburg, IL) at 30 kV. The images (1280 × 960 pixels) were acquired using a Gatan high-angle annular bright field (HAABF) scintillating detector. Measurements were performed at a magnifications of 200 000 (200 k ×), with a pixel size of 0.331 nm and micron marker of 100.

Dynamic Light Scattering (DLS) Measurements. The hydrodynamic sizes of BSA and Que-loaded BSA NP were determined by means of photon correlation spectroscopy using a Delsa Nano Particle Analyzer (A53878, Beckman Coulter, Inc., Brea, CA). The concentration of BSA was set at 1.5×10^{-5} mol/L. The size measurement was performed at 25 °C and at a 15° scattering angle. It was recorded for 400 μs for each measurement, and the accumulation time was three times. When the hydrodynamic size was measured in DLS, the fluctuations in time of scattered light from particles in Brownian motion were measured.

Circular Dichroism (CD) Measurements. The CD spectra of BSA and Que-loaded BSA NP were recorded using a Jasco-720 spectropolarimeter (Jasco Products Co., Oklahoma City, OK). The concentration of BSA was set at 1.5×10^{-5} mol/L. For measurements in the near-UV region (250−330 nm), a quartz cell with a path length of 1 cm was used in nitrogen atmosphere. An accumulation of five scans with time per point of 2.5 s was performed, and data were collected for each nanometer from 330 to 250 nm. A reference sample containing Milli-Q water and DMSO was subtracted from the CD signal for measurements.

Three-Dimensional Fluorescence Spectrometry. The three-dimensional fluorescence spectra of BSA, Que, and Que-loaded BSA NP solutions were recorded by a Cary Eclipse fluorophotometer (Varian, Inc., CA) equipped with 1.0 cm quartz cells. The concentration of BSA was set at 1.5×10^{-5} mol/L and that of Que at 1.5×10^{-4} mol/L. The widths of the excitation and emission slits were set to 2.5 and 5.0 nm, respectively. The emission wavelength was recorded between 200 and 600 nm, and the excitation wavelength was set from 200 to 600 nm with an increment of 5 nm; the number of scanning curves was 15 times.

Simulated Intestinal Fluid (SIF) Stability Assay. The stability of free and encapsulated Que was investigated within 6 h in SIF. The concentration of Que was set at 1.5×10^{-4} mol/L and that of BSA at 1.5×10^{-5} mol/L. SIF was prepared as described in the United States Pharmacopoeia[11] and consisted of 1% of pancreatin in 0.05 M KH_2PO_4, pH 7.4. The test sample solution and SIF (absence or presence of pancreatin) were mixed in 50 mL microcentrifuge tubes and then were incubated at 37 °C. At intervals of 0, 1, 2, 3, 4, 5, and 6 h, 2 mL of solution was taken out and analyzed by means of UV−vis spectrometry as described below.

UV−Vis Spectrometry. The sample solutions of free and encapsulated Que were scanned on a Varian Cary 50 UV−vis spectrophotometer (Varian Medical Systems, Inc., Palo Alto, CA) with the wavelength range of 300−500 nm. The concentration of Que was set at 1.5×10^{-5} mol/L and that of BSA at 1.5×10^{-5} mol/L. The operations were carried out at room temperature (25 °C). The scan rate was 600 nm/min. The data interval was 1 nm, and average time was 0.10 s.

Antioxidant Activity Evaluation. The antioxidant activity of free and encapsulated Que was evaluated by DPPH and ABTS assays. The concentration of Que was set at 1.5×10^{-5} mol/L and that of BSA at 0, 0.15×10^{-5}, 0.75×10^{-5}, and 1.5×10^{-5} mol/L.

DPPH Assay. The DPPH free radical scavenging activity was determined according to the method of Jing and Kitts.[12] Stock solutions of DPPH$^{\bullet}$ were prepared at 2.5 mmol/L and then diluted to 0.15 mmol/L. Each sample (15 μL) was mixed with 0.05 mol/L (pH 7.4) Tris-HCl buffer (60 μL) and 0.15 mmol/L DPPH$^{\bullet}$ working solution (150 μL) in a 96-well plate. The mixture was shaken vigorously and then left to stand for 30 min in the dark. The absorbance (A_{sample}) at 517 nm was recorded using a microplate reader (model 680, Bio-Rad Laboratories, Inc., Hercules, CA). All of the samples were analyzed in triplicate. The absorbance of the control ($A_{control}$) was obtained by replacing the sample with ethanol. The DPPH radical scavenging activity (RSA) was calculated using eq 1:

$$\text{RSA}\ (\%) = [(A_{control} - A_{sample})/A_{control}] \times 100\% \qquad (1)$$

ABTS Assay. The experiment was carried out using an improved ABTS decoloration assay of Jing and Kitts.[12] Briefly, 140 mmol/L ABTS stock solution was diluted in water to 14 mM concentration. Five hundred microliters of 14 mM ABTS dilution and 500 μL of 4.9 mM potassium persulfate (KPS) stock solution were mixed in a 1.5 mL tube and then left to stand in the dark and at room temperature for at least 12 h. The ABTS$^{\bullet}$ was then diluted with sample buffer to an absorbance of 0.700 ± 0.020 at 734 nm before use. After the addition of 900 μL of diluted ABTS$^{\bullet}$ solution to 100 μL of samples, the absorbance of sample (A_{sample}) reading was taken exactly after 4 min, and the absorbance of sample buffer blank ($A_{control}$) was run in each assay. The absorbance at 734 nm was recorded by means of UV−vis spectrometry. All determinations were carried out in triplicate. The ABTS RSA was also calculated using eq 1.

Statistical Analysis. All experiments were performed in triplicate. The data were presented as the mean ± SD. Means were compared by one-way ANOVA, followed by Tukey's pairwise comparisons, using Minitab software (Minitab Inc., State College, PA). The level of confidence required for significance was set at $p < 0.05$.

RESULTS

Morphology and Size Measurements. STEM and DLS were combined to analyze the size and conformational features of the BSA NP as shown in Figure 1. Without DMSO and Que, STEM micrographs (Figure 1A) showed that BSA molecules were cross-linked and formed loose aggregates. Meanwhile, DLS data showed two size distributions in the solution (Figure 1A′), where the smaller size was about 2 nm and the bigger one about 15 nm. It was reported that the BSA molecule in water had an ellipsoidal shape (14 nm long and 4 nm short axis).[13] In our case, the smaller size was a fragment of BSA molecule, and the bigger size was the individual BSA molecule. When DMSO was 10% and Que was 1.5×10^{-4} mol/L, compact and quasi-spherical aggregates occurred (Figure 1B), with the particle size <10 nm (Figure 1B′).

Stability of Que in SIF. Que has maximum absorption at 365 nm owing to its chromophoric group, and the absorptions (Abs) at 365 nm are proportionate to the concentration of Que in the solution. UV−vis spectrometry was used to detect the concentration variety of Que in the absence or presence of BSA NP. As shown in Figure 2, the concentration of free Que decreased >60% within 6 h, whereas no decrease was observed

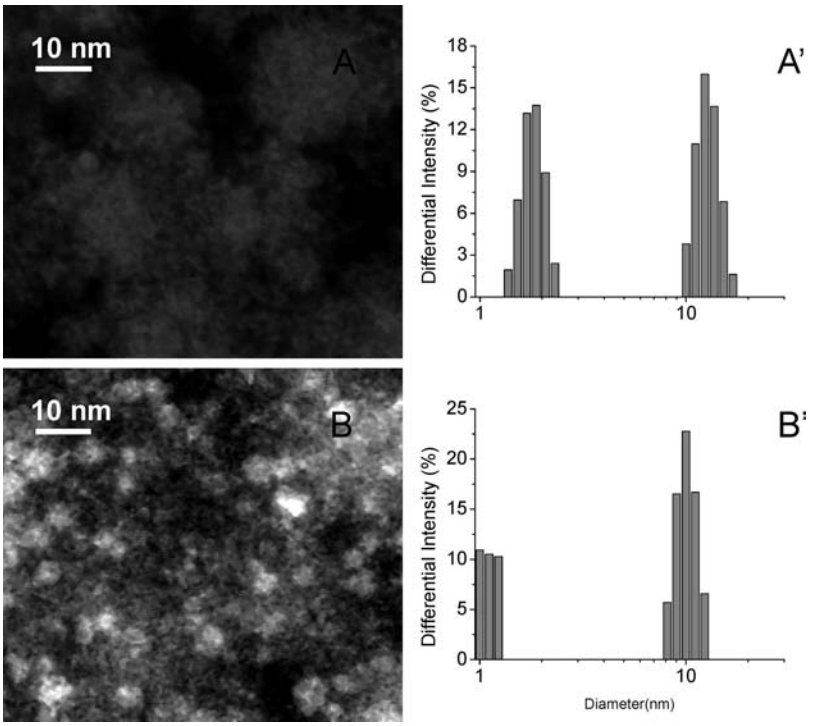

Figure 1. STEM images of native BSA (A) and Que-loaded BSA NP (B) and size distribution histograms of BSA (A′) and Que-loaded BSA NP (B′). (A) $C_{BSA} = 1.5 \times 10^{-5}$ mol/L, $C_{Que} = 0$ mol/L, (A′) $C_{BSA} = 1.5 \times 10^{-5}$ mol/L, $C_{Que} = 0$ mol/L, (B) $C_{BSA} = 1.5 \times 10^{-5}$ mol/L, $C_{Que} = 1.5 \times 10^{-4}$ mol/L, (B′) $C_{BSA} = 1.5 \times 10^{-5}$ mol/L, $C_{Que} = 1.5 \times 10^{-4}$ mol/L.

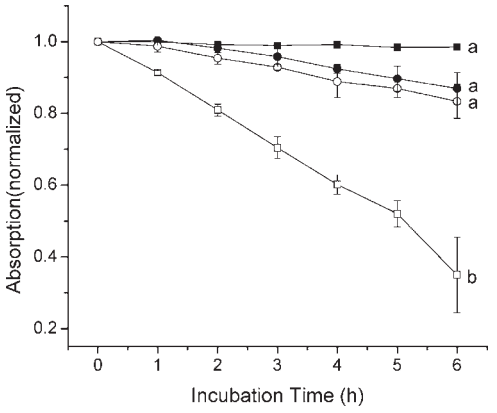

Figure 2. Stability of free and encapsulated Que within 6 h at 37 °C: □, free Que in SIF (absence of pancreatin), $C_{BSA} = 0$ mol/L, $C_{Que} = 1.50 \times 10^{-4}$ mol/L; ■, encapsulated Que in SIF (absence of pancreatin), $C_{BSA} = 1.50 \times 10^{-5}$ mol/L, $C_{Que} = 1.50 \times 10^{-4}$ mol/L; ○, free Que in SIF (presence of pancreatin), $C_{BSA} = 0$ mol/L, $C_{Que} = 1.50 \times 10^{-4}$ mol/L; ●, encapsulated Que in SIF (presence of pancreatin), $C_{BSA} = 1.50 \times 10^{-5}$ mol/L, $C_{Que} = 1.50 \times 10^{-4}$ mol/L. Values were expressed as relative absorption at 365 nm (in % of $t = 0$). Different letters in the figure denote that the mean difference is significant at $p < 0.05$.

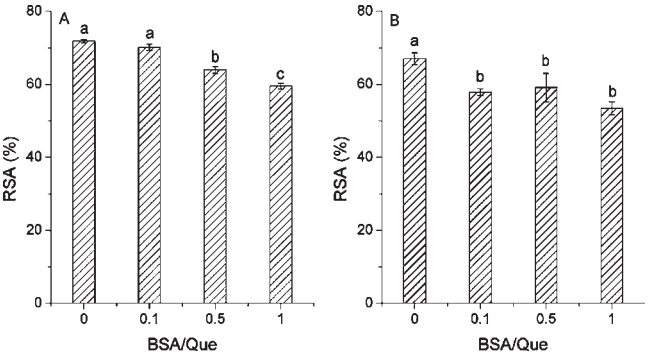

Figure 3. DPPH (A) and ABTS (B) scavenging activity of free and encapsulated Que. $C_{Que} = 1.50 \times 10^{-5}$ mol/L: $C_{BSA} = 0$, 0.15×10^{-5}, 0.75×10^{-5}, and 1.50×10^{-5} mol/L. The DPPH and ABTS scavenging activities of BSA were subtracted from the encapsulated Que. The BSA/Que in the *x*-axis represents the molar ratio of BSA and Que in the system. Markers of different letters in the figure denote that the mean difference is significant at $p < 0.05$.

in the case of encapsulated Que in SIF (in the absence of pancreatin). However, the concentrations of free and encapsulated Que decreased at a similar degree of 15% in SIF (in the presence of pancreatin).

Antioxidant Activity of Que. DPPH and ABTS radical cation decolorization tests were widely used for the assessment of the antioxidant activity of various substances. Previous works confirmed that Que had great DPPH and ABTS antioxidant activity.[14,15] Ghanta[15] reported that the 50% inhibitory concentration (IC_{50}) values of Que for DPPH and ABTS scavenging were 3.35 ± 0.07 and 1.30 ± 0.06 μg/mL, respectively. In the present test, the concentration of Que was set at 1.5×10^{-5} mol/L. As shown in Figure 3A, the DPPH RSA (%) for free Que was 71.86%, and those for the Que encapsulated by 0.15×10^{-5}, 0.75×10^{-5}, and 1.5×10^{-5} mol/L BSA NP were 70.22, 63.97, and 59.50%, respectively. The BSA NP decreased ($p < 0.05$) the DPPH RSA (%) of Que. In the case of the ABTS assay (Figure 3B), the ABTS RSA (%) for free Que was 67.06%, and

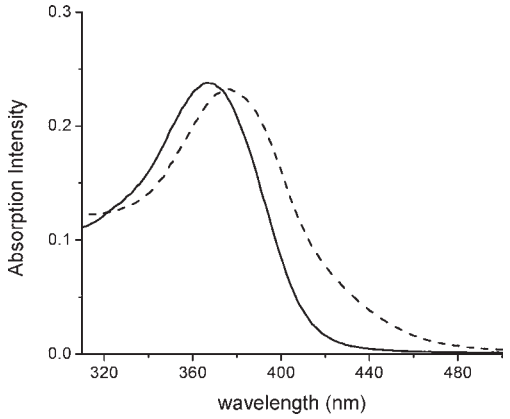

Figure 4. UV−vis absorption of the free (solid) and encapsulated (dash) Que. The BSA absorption signal was subtracted. C_{Que} = 1.5 × 10^{-5} mol/L; C_{BSA} = 0 and 1.5 × 10^{-5} mol/L.

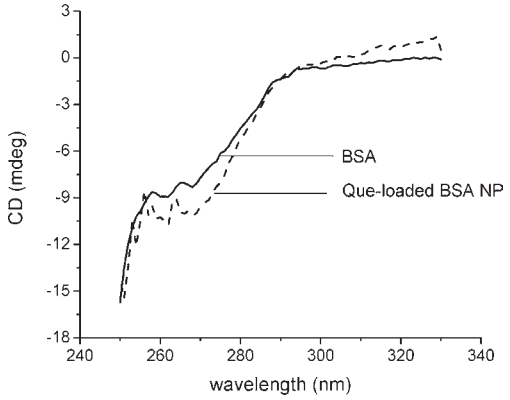

Figure 5. Near-UV CD spectra of native BSA and Que-loaded BSA NP. C_{BSA} = 1.50 × 10^{-5} mol/L; C_{Que} = 0 and 1.50 × 10^{-4} mol/L.

those for the Que encapsulated by 0.15 × 10^{-5}, 0.75 × 10^{-5}, and 1.5 × 10^{-5} mol/L BSA NP were 57.89, 59.15, and 53.45%, respectively, indicating BSA NP decreased (p < 0.05) the ABTS RSA (%) of Que.

UV−Vis Spectrum. The absorption spectrum of Que at 300−500 nm usually has one band, which is associated with the cinnamoyl group (B- and C-rings of Que).[10] The UV−vis spectra of the free and encapsulated Que are compared in Figure 4. The characteristic band of Que was at 365 nm (solid line). However, a red shift of 12 nm of the band was observed in the case of BSA NP encapsulated Que (dash line).

CD Spectrum. CD was used to monitor the conformational changes of the protein. The $\pi-\pi^*$ transitions of aromatic acids side chains contributed to near-UV protein CD (250−330 nm), so the change of near-UV CD signal was used as an indicator of tertiary interactions. Generally, the absorption intensity around 290−295 nm represents the Trp content.[16,17] A broad positive CD band was observed in the range of 250−270 nm, and the position of this band as well as the absence of fine structure suggested the contribution of disulfide chromophores.[18] The CD spectra (250−330 nm) of the BSA and Que-loaded BSA were compared (Figure 5). They showed an ellipticity decrease in the region between 250 and 270 nm and an ellipticity rise in the region between 290 and 295 nm when BSA was loaded with Que.

Three-Dimensional Fluorescence Spectrum. A three-dimensional fluorescence spectrum can exhibit comprehensive fluorescence information of the sample.[19,20] The three-dimensional fluorescence spectra of BSA (A), Que (B), and Que-loaded BSA NP (C) are shown in Figure 6. Peak a is the Rayleigh scattering peak ($\lambda_{ex} = \lambda_{em}$), and the intensity represents the scale of particle. The fluorescence intensity of peak a decreased in the presence of Que (Figure 6C; Table 1), indicating a more compact complex formation. Peak 1 (λ_{ex} = 283.0 nm, λ_{em} = 343.0 nm) mainly reveals the spectral behavior of Trp residues of BSA. When BSA is excited at 283 nm, the intrinsic fluorescence reveals mainly both Trp and tyrosine (Tyr) residues, but the Tyr emission at 304 nm yields a fairly low quantum,[21,22] and thus the intensity of Tyr at 344 nm can be negligible. The fluorescence intensities of peak 1 decreased obviously as in the presence of Que (Figure 6C; Table 1). The decrease demonstrated that Que interacted with BSA and resulted in fluorescence quenching of BSA. A new peak (peak 2) appeared in the presence of Que (Figure 6C), but not with only free Que (Figure 6B).

DISCUSSION

Self-Assembly of Que-Loaded BSA NP. The BSA molecule has an ellipsoidal shape of 14 nm long and 4 nm short axis in water and can aggregate to form loose micelles through the hydrophobic interaction between the nonpolar parts of the molecules.[23,24] When Que and DMSO were present, a self-assembly of BSA NP formed and became smaller and more compact in comparison with native BSA. This was supported by the near-UV CD spectra of BSA. A rise in ellipticity (290−295 nm) and a decrease in ellipticity (250−270 nm) were observed in the presence of Que. The ellipticity change from 250 to 270 nm reflected the perturbations around disulfide bridges, which in turn resulted in the change of tertiary structure.[18,25] The binding capacity of BSA NP to Que had been calculated in our previous work, and the result showed that 1 BSA molecule could encapsulate 11 Que molecules.[26] In this study, we compared for the first time the stability and antioxidant activity of free and encapsulated Que and evaluated the effects of BSA NP on Que stability. Moreover, the mechanism of Que stabilization was investigated.

Influences of BSA NP on the Stability and Antioxidant Activity of Que. Que is chemically unstable in aqueous alkaline medium, due to its fast autoxidation with O_2 and the formation of *o*-quinone/quinone methide (QQ).[2,3] Our results showed that the concentration of Que did not decrease in SIF when it was encapsulated by BSA NP, which indicated that the oxidation process of Que was apparently prevented by the BSA NP. However, the protection was hampered due to the enzymolysis of BSA by pancreatin. It is worth noting that Que was also protected by protease, but the protection was weaker with protease than with BSA NP. Que demonstrated strong scavenging activity for DPPH and ABTS radicals, which was attributed to its phenolic hydroxyl groups. The antioxidant activity of Que could vanish when its phenolic hydroxyl groups were blocked by interaction.[27] However, our results indicated that the antioxidant activity of encapsulated Que did not decrease substantially. That is to say, the majority of phenolic hydroxyl groups do not participate in the interaction of Que and BSA NP.

Interaction between Que and BSA. It was previously reported that interaction between BSA and Que was through hydrophobic association or hydrogen bond.[9,10] This was in

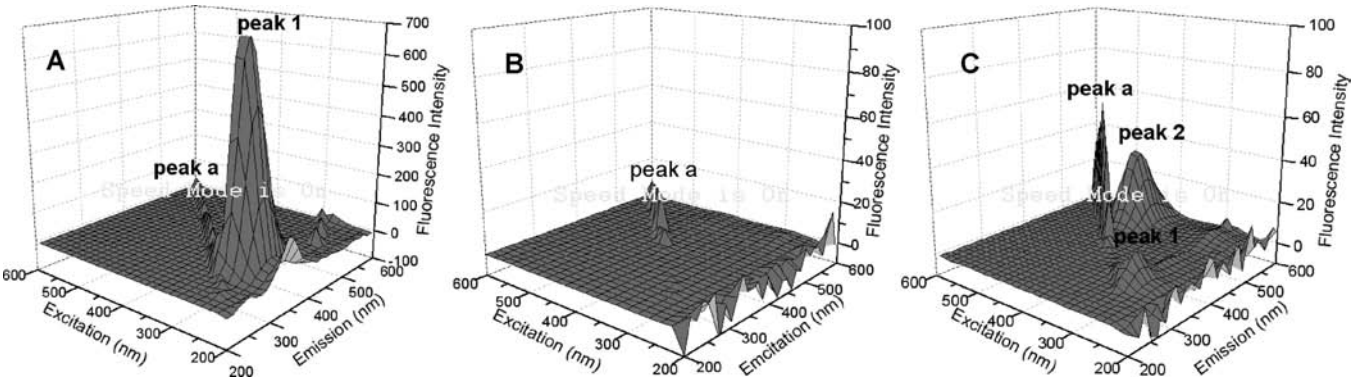

Figure 6. Three-dimensional fluorescence spectra of BSA (A), Que (B), and Que-loaded BSA NP (C). (A) C_{BSA}= 1.5 × 10^{-5} mol/L; C_{Que} = 0 mol/L. (B) C_{BSA} = 0 mol/L; C_{Que} = 1.5 × 10^{-4} mol/L. (C) C_{BSA}= 1.5 × 10^{-5} mol/L; C_{Que} = 1.5 × 10^{-4} mol/L. pH 7.00, t = 25 °C.

Table 1. Characteristic Three-Dimensional Fluorescence Spectral Data of BSA, Que, and Que-Loaded BSA NP System

	BSA		Que		Que-loaded BSA NP	
peak	position ($\lambda_{ex}/\lambda_{em}$, nm)	intensity	position ($\lambda_{ex}/\lambda_{em}$, nm)	intensity	position ($\lambda_{ex}/\lambda_{em}$, nm)	intensity
a		74.4		14.5		60.4
1	283/343	750.4			289/332	14.0
2					454/534	37.4

conformity with our results. The near-UV CD spectroscopy of BSA revealed an ellipticity rise in the region between 290 and 295 nm in the presence of Que, which was ascribed to the increase of hydrophobicity on Trp residues. The fluorescence and Raman measurements also confirmed the hydrophobic association between Que and BSA (data not shown). In addition to the hydrophobic association, the hydrogen bond participated in the interaction between Que and BSA. It was observed that a bathochromic shift of UV−vis spectrum occurred as Que was encapsulated by BSA NP. Que has maximum absorption at 365 nm owing to its chromophoric group. If the hydrogen bonding has occurred between the chromophoric group and some auxochromic group, such as −OH, $-NH_2$, −SH, −Cl, −OR, or −SR, the lone-pair electrons in the auxochromic group will conjugate with the chromophoric group. This leads to a decrease of the $\pi-\pi$ transition energy with the bathochromic shift.[28,29] It could be concluded that a hydrogen bond formed between Que and BSA. This was in accordance with the variation trend of three-dimensional fluorescence spectra between free and encapsulated Que. Que is a flavonol that possesses hydroxy groups at the 3- and 5-positions. The 3-hydroxyflavone (3-HF) readily yields an excited state intramolecular proton transfer (ESIPT), exhibiting a strongly shifted PT fluorescence green in nonprotic solvents (i.e., DMSO). However, the 5-hydroxyflavone (5-HF) constitutes the special class of nonfluorescent flavonol resulting from the formation of a strong intramolecular hydrogen bond between the 5-OH group and the carbonyl oxygen. This pathway was explained by formation of a pseudo-Jahn−Teller distorted excited state due to near degeneracy of π,π^* and n,π^* states of 5-HFs. As a result, the fluorescence emission intensity of Que was so slight that it could not be detected. However, it showed that interaction of BSA caused a dramatic enhancement in the fluorescence emission intensity of Que at ESPT tautomer (green) bands, characteristic of the compound 3-HF (peak 2, λ_{ex} = 454.0 nm, λ_{em} = 534.0 nm).[10] These observations can be rationalized as the intramolecular hydrogen bond of 5-OH to the neighboring carbonyl group of Que being interrupted and transformed to an intermolecular hydrogen bond between 5-OH and a group of BSA. A residual intramolecular hydrogen bond of the 3-OH group to the carbonyl remains.[30,31]

Mechanism of Quercetin Stabilization. The synergy of DMSO and Que resulted in the formation of compact BSA NP through micellization and protein folding. Thus, Que was wrapped in the hydrophobic core of the BSA NP, and the compact microstructure hampered the transfer of O_2 from water to the core of BSA NP. In addition, the intermolecular hydrogen bond between BSA and Que might also contribute to Que stabilization. The strength of the intramolecular hydrogen bond of the 5-OH and 3-OH groups to the neighboring carbonyl group could be attributed to the greater resonance stabilization, due to the formation of a six-membered ring.[32,33] As Que is encapsulated by BSA NP, the intermolecular hydrogen bond has been formed between 5-OH group and BSA. It was inferred that the intermolecular hydrogen bond might be more favorable for the stabilization of Que than the intramolecular hydrogen bond. Our previous work[26] showed that Que was not protected effectively by lysozyme and myoglobin NP as the hydrogen bond did not participate in the interaction between Que and lysozyme or myglobin NP. This suggested that the hydrogen bond formation was important to the mechanism of Que stabilization.

It has been shown that the antioxidant activity of Que slightly decreased as it bound to BSA. The −OH moieties of the Que were very important for antioxidant activity, such as 5,7-dihydroxylation at the A-ring, 3′,4′-dihydroxylation at the B-ring, and 3-hydroxylation at the C-ring. The 5-OH at the A-ring formed an intermolecular hydrogen bond with BSA, and thus the antioxidant activity decreased slightly. Nevertheless, the −OH moieties of the B-ring, the most significant factor in the scavenging of

reactive oxygen species, were not involved in the interaction, and accordingly the antioxidant activity was not substantially decreased.

In summary, Que was encapsulated by BSA NP through hydrophobic interaction and hydrogen bonding. The size of spherical Que-loaded BSA NP is <10 nm. BSA NP can effectively promote the stability of Que in SIF, and the antioxidant activity of encapsulated Que has also been preserved. Although the hydrophobic interaction contributes to stabilizing Que, the hydrogen bond is the crux of the matter.

AUTHOR INFORMATION

Corresponding Author

*Phone: + 86-10-6273-7909. Fax: + 86-10-6273-7909. E-mail: hao.haojing@gmail.com.

ACKNOWLEDGMENT

Prof. Guanghua Zhao (College of Food Science and Nutritional Engineering, China Agricultural University, Beijing, China), Prof. Yunjie Yan (Beijing National Center for Microscopy, Tsinghua University, Beijing, China), and Prof. Wei Qi (Chemical Engingeeing Research Center School of Chemical Engingeering and Technology Tianjin University, Tianjin, China) are acknowledged for their technical advice.

ABBREVIATIONS USED

BSA, bovine serum albumin; Que, quercetin; NP, nanoparticle; STEM, scanning transmisson electron microscopy; DLS, dynamic light scattering; CD, circular dichroism; Trp, tryptophan; Tyr, tyrosine; DMSO, dimethyl sulfoxide; DPPH, 2,2-diphenyl-1-picrylhydrazyl; ABTS, 3-ethylbenzothiazoline-6-sulfonic acid; SIF, simulated intestinal fluid.

REFERENCES

(1) Di Carlo, G.; Mascolo, N.; Izzo, A.; Capasso, F. Flavonoids: old and new aspects of a class of natural therapeutic drugs. *Life Sci.* **1999**, *65*, 337–353.

(2) van der Woude, H.; Gliszczyska-wigo, A.; Struijs, K.; Smeets, A.; Alink, G.; Rietjens, I. Biphasic modulation of cell proliferation by quercetin at concentrations physiologically relevant in humans. *Cancer Lett.* **2003**, *200*, 41–47.

(3) Makris, D.; Rossiter, J. Heat-induced, metal-catalyzed oxidative degradation of quercetin and rutin (quercetin 3-*O*-rhamnosylglucoside) in aqueous model systems. *J. Agric. Food Chem.* **2000**, *48*, 3830–3838.

(4) Musthaba, S.; Baboota, S.; Ahmed, S.; Ahuja, A.; Ali, J. Status of novel drug delivery technology for phytotherapeutics. *Expert Opin. Drug Deliv.* **2009**, *6*, 625–637.

(5) Maghsoudi, A.; Shojaosadati, S.; Vasheghani Farahani, E. 5-Fluorouracil-loaded BSA nanoparticles: formulation optimization and in vitro release study. *AAPS Pharm. Sci. Technol.* **2008**, *9*, 1092–1096.

(6) Ascenzi, P.; Bocedi, A.; Notari, S.; Fanali, G.; Fesce, R.; Fasano, M. Allosteric modulation of drug binding to human serum albumin. *Mini−Rev. Med. Chem.* **2006**, *6*, 483–489.

(7) Swaney, J.; Klotz, I. Amino acid sequence adjoining the lone tryptophan of human serum albumin. A binding site of the protein. *Biochemistry* **1970**, *9*, 2570–2574.

(8) Fasano, M.; Curry, S.; Terreno, E.; Galliano, M.; Fanali, G.; Narciso, P.; Notari, S.; Ascenzi, P. The extraordinary ligand binding properties of human serum albumin. *IUBMB Life* **2005**, *57*, 787–796.

(9) Dufour, C.; Dangles, O. Flavonoid−serum albumin complexation: determination of binding constants and binding sites by fluorescence spectroscopy. *Biochim. Biophys. Acta* **2005**, *1721*, 164–173.

(10) Ni, Y.; Zhang, X.; Kokot, S. Spectrometric and voltammetric studies of the interaction between quercetin and bovine serum albumin using warfarin as site marker with the aid of chemometrics. *Spectrochim. Acta A: Mol. Biomol. Spectrosc.* **2009**, *71*, 1865–1872.

(11) *23, National Formulary 18*; U.S. Pharmacopeia: Rockville, MD, 1995; pp 2299−2300.

(12) Jing, H.; Kitts, D. Antioxidant activity of sugar−lysine maillard reaction products in cell free and cell culture systems. *Arch. Biochem. Biophys.* **2004**, *429*, 154–163.

(13) Ou, W.; Wang, R.; Zhou, H. Conformational changes and inactivation of rabbit muscle creatine kinase in dimethyl sulfoxide solutions. *Biochem. Cell Biol.* **2002**, *80*, 427–434.

(14) Ozgen, M.; Reese, R.; Tulio, A., Jr.; Scheerens, J.; Miller, A. Modified 2,2-azino-bis-3-ethylbenzothiazoline-6-sulfonic acid (ABTS) method to measure antioxidant capacity of selected small fruits and comparison to ferric reducing antioxidant power (FRAP) and 2, 2′-diphenyl-1-picrylhydrazyl (DPPH) methods. *J. Agric. Food Chem.* **2006**, *54*, 1151–1157.

(15) Ghanta, S.; Banerjee, A.; Poddar, A.; Chattopadhyay, S. Oxidative DNA damage preventive activity and antioxidant potential of *Stevia rebaudiana* (Bertoni) Bertoni, a natural sweetener. *J. Agric. Food Chem.* **2007**, *55*, 10962–10967.

(16) Liang, J.; Chakrabarti, B. Spectroscopic investigations of bovine lens crystallins. 1. Circular dichroism and intrinsic fluorescence. *Biochemistry* **1982**, *21*, 1847–1852.

(17) Sreerama, N.; Woody, R. Computation and analysis of protein circular dichroism spectra. *Methods Enzymol.* **2004**, *383*, 318–351.

(18) Sun, C.; Yang, J.; Wu, X.; Huang, X.; Wang, F.; Liu, S. Unfolding and refolding of bovine serum albumin induced by cetylpyridinium bromide. *Biophys. J.* **2005**, *88*, 3518–3524.

(19) Lu, X.; Fan, J.; Liu, Y.; Hou, A. Characterization of the interaction between cationic erbium(III)−porphyrin complex with bovine serum albumin. *J. Mol. Struct.* **2009**, *934*, 1–8.

(20) Ding, F.; Han, B.; Liu, W.; Zhang, L.; Sun, Y. Interaction of imidacloprid with hemoglobin by fluorescence and circular dichroism. *J. Fluoresc.* **2010**, *20*, 753–762.

(21) Graziani, M.; Finazzi-Agro, A.; Rotillo, G.; Barra, D.; Mondovi, B. Parsley plastocyanin. Possible presence of sulfhydryl and tyrosine in the copper environment. *Biochemistry* **1974**, *13*, 804–809.

(22) Kimura, T.; Nagata, Y.; Tsurugi, J. Studies on adrenal steroid hydroxylases. *J. Biol. Chem.* **1970**, *245*, 4450–4452.

(23) Kandori, K.; Toshima, S.; Wakamura, M.; Fukusumi, M.; Morisada, Y. Effects of modification of calcium hydroxyapatites by trivalent metal ions on the protein adsorption behavior. *J. Phys. Chem. B* **2010**, *114*, 2399–2404.

(24) Giovambattista, N.; Lopez, C.; Rossky, P.; Debenedetti, P. Hydrophobicity of protein surfaces: separating geometry from chemistry. *Proc. Natl. Acad. Sci. U.S.A.* **2008**, *105*, 2274.

(25) Wu, D.; Xu, G.; Sun, Y.; Zhang, H.; Mao, H.; Feng, Y. Interaction between proteins and cationic gemini surfactant. *Biomacromolecules* **2007**, *8*, 708–712.

(26) Fang, R.; Jing, H.; Chai, Z.; Zhao, G. H.; Stoll, S.; Ren, F. Z.; Liu, F.; Leng, X. J. Design and characterization of protein−quercetin bioactive nanoparticles. *J. Nanobiotechnol.* **2011**, in press.

(27) Xiao, J.; Suzuki, M.; Jiang, X.; Chen, X.; Yamamoto, K.; Ren, F.; Xu, M. Influence of B-ring hydroxylation on interactions of flavonols with bovine serum albumin. *J. Agric. Food Chem.* **2008**, *56*, 2350–2356.

(28) Würthner, F.; Chen, Z.; Hoeben, F.; Osswald, P.; You, C.; Jonkheijm, P.; Herrikhuyzen, J.; Schenning, A.; van der Schoot, P.; Meijer, E. Supramolecular *p-n*-heterojunctions by co-self-organization of oligo (*p*-phenylene vinylene) and perylene bisimide dyes. *J. Am. Chem. Soc.* **2004**, *126*, 10611–10618.

(29) Bell, T.; Hext, N. Supramolecular optical chemosensors for organic analytes. *Chem. Soc. Rev.* **2004**, *33*, 589–598.

(30) Sengupta, B.; Sengupta, P. The interaction of quercetin with human serum albumin: a fluorescence spectroscopic study. *Biochem. Biophys. Res. Commun.* **2002**, *299*, 400–403.

(31) Sengupta, B.; Sengupta, P. Binding of quercetin with human serum albumin: a critical spectroscopic study. *Biopolymers* **2003**, *72*, 427–434.

(32) van Acker, S.; de Groot, M.; van den Berg, D.; Tromp, M.; den Kelder, G.; van der Vijgh, W.; Bast, A. A quantum chemical explanation of the antioxidant activity of flavonoids. *Chem. Res. Toxicol.* **1996**, *9*, 1305–1312.

(33) Exarchou, V.; Troganis, A.; Gerothanassis, I.; Tsimidou, M.; Boskou, D. Do strong intramolecular hydrogen bonds persist in aqueous solution? Variable temperature gradient ^{1}H, $^{1}H-^{13}C$ GE-HSQC and GE-HMBC NMR studies of flavonols and flavones in organic and aqueous mixtures. *Tetrahedron* **2002**, *58*, 7423–7429.